Biochemical and Biophysical Research Communications 437 (2013) 482–488

Contents lists available at SciVerse ScienceDirect

Biochemical and Biophysical Research Communications

journal homepage: www.elsevier.com/locate/ybbrc

Proteomics analysis of autophagy-deficient Atg7$^{-/-}$ MEFs reveals a close relationship between F-actin and autophagy

Cuiqin Zhuo [a,b,1], Yuhua Ji [c,1], Zhenping Chen [b,*], Kaio Kitazato [d], Yangfei Xiang [a,b], Meigong Zhong [a,b], Qiaoli Wang [b], Ying Pei [b], Huaiqiang Ju [b], Yifei Wang [b,*]

[a] College of Pharmacy, Jinan University, Guangzhou, China
[b] Biomedicine Research and Development Center of Jinan University, Guangzhou, Guangdong 510632, China
[c] Institute of Tissue Transplantation and Immunology, College of Life Science and Technology, Jinan University, Guangzhou 510632, China
[d] Division of Molecular Pharmacology of Infectious Agents, Department of Molecular Microbiology and Immunology, Graduate School of Biomedical Sciences, Nagasaki University, Nagasaki 852-8521, Japan

ARTICLE INFO

Article history:
Received 26 June 2013
Available online 9 July 2013

Keywords:
Proteomics analysis
Autophagy-deficient MEFs
Atg7
F-actin

ABSTRACT

Autophagy plays a crucial role in a wide array of physiological processes. To uncover the complex regulatory networks and mechanisms underlying basal autophagy, we performed a quantitative proteomics analysis of autophagy-deficient mouse embryonic fibroblast cells (MEFs) using iTRAQ labeling coupled with on-line 2D LC/MS/MS. We quantified a total of 1234 proteins and identified 114 proteins that were significantly altered (90% confidence interval), including 48 up-regulated proteins and 66 down-regulated proteins. We determined that F-actin was disassembled in autophagy-deficient Atg7$^{-/-}$ MEFs. Treatment of the WT MEFs with cytochalasin D (CD), which induces F-actin depolymerization, significantly induced autophagosome formation. However, treatment with cytochalasin D also increased the protein level of p62 under starvation conditions, suggesting that depolymerization of F-actin impaired autophagosome maturation and that the intact F-actin network is required for basal and starvation-induced autophagy. Our results demonstrate a close relationship between F-actin and autophagy and provide the basis for further investigation of their interactions.

1. Introduction

The autophagy process is an evolutionarily conserved degradative pathway in eukaryotic cells [1]. Autophagy involves a series of steps, including induction, cargo recognition and assembly, vesicle nucleation, vesicle dilation and completion, vesicle fusion with the lysosome/vacuole, vesicle disintegration, and reutilization of the resulting macromolecules[2]. Autophagy is also associated with a wide array of physiological processes, such as immunity [3], development [4], and cell death [5]. Impaired autophagy causes the accumulation of abnormal proteins, interferes with normal cellular functions [6,7], and triggers several pathological conditions, including certain malignancies, Huntington's disease, Parkinson's disease, and Alzheimer's disease [8].

The autophagy pathway is complex; genetic analysis of *Saccharomyces cerevisiae* has identified over 30 genes related to autophagy todate (*ATG*; autophagy-related gene) [9]. A number of specific *ATG*s constitute two ubiquitin-like conjugation systems, the *ATG8* and *ATG12* conjugation systems [10,11]. Atg7p (an E1-like enzyme) activates Atg12p [12], which is later transferred to the E2-like enzyme Atg10p and subsequently conjugated to Atg5p. Similar to Atg12p, Atg8p is activated by Atg7p and transferred to the E2-like enzyme Atg3p [11]. Mammals express at least three Atg8 homologues: GABARAP, GATE-16, and LC3. The *ATG7* gene encodes the E1-like enzyme Atg7p, which is involved specifically in autophagosome formation and is indispensable for autophagy [13]. Therefore, the *ATG7* gene is essential in the autophagy process.

To characterize the overall protein dynamics of basal autophagy further, we applied iTRAQ labeling coupled with on-line 2D LC/MS/MS proteomics technology [14] to perform the first large-scale analysis of the protein expression profile of Atg7$^{-/-}$ MEFs derived from Atg7-knockout mice [15,16]. We quantified 1234 proteins and identified 114 significantly altered proteins (90% confidence interval). The ingenuity pathway analysis (IPA) of the network demonstrated that filamentous actin (F-actin) was an important hub in the protein–protein interaction network. We confirmed that autophagy impairment induced by Atg7 deficiency affected the morphology of F-actin in the MEFs. Experiments performed in CD-treated WT MEFsdemonstrated that depolymerization of F-actin might impair autophagosome maturation during basal and starvation-induced autophagy. In summary, our data suggest that F-actin is closely associated with autophagy, and further investigation of the mechanisms

* Corresponding authors. Fax: +86 20 85223426.
E-mail addresses: 530670663@qq.com (Z. Chen), twang-yf@163.com (Y. Wang).
[1] These authors contributed equally to this work.

0006-291X/$ - see front matter © 2013 Elsevier Inc. All rights reserved.
http://dx.doi.org/10.1016/j.bbrc.2013.06.111

by which F-actin polymerization interacts with the autophagy process is warranted.

2. Materials and methods

2.1. Cell culture and reagents

The immortalized WT and Atg7-deficient mouse embryonic fibroblast cells (WT MEFs and Atg7$^{-/-}$ MEFs) were generously provided by Dr. Masaaki Komatsu (Tokyo Metropolitan Institute of Medical Science) [15,16]. The cells were propagated in modified Eagle's medium (MEM; Invitrogen, 41500–034) supplemented with 10% fetal bovine serum (FBS; Gibco, 8172879) at 37 °C in a humidified atmosphere containing 5% (v/v) CO_2. The medium was changed every 2 days. The reagents used in this study were as follows: cytochalasin D (final concentration 2 μM; Gibco, PHZ1063), tetramethylrhodamine B isothiocyanate (TRITC)-phalloidin (5 μM; Sigma–Aldrich, P1951), 4′,6′-diamidino-2-phenylindole (DAPI, 1 mg/mL; Biotium, 40011), and monodansylcadaverine (MDC, 50 μM; Sigma–Aldrich, 30432).

2.2. Western blotting

Cells were lysed in RIPA buffer (Beyotime, P0013B) containing 1% PMSF (Beyotime, ST506) and clarified by centrifugation at 15,000×*g* for 15 min at 4 °C. The protein concentration in the supernatant was measured using the BCA protein assay kit (Beyotime, P0010) [17]. The cell lysates were mixed with 5× SDS–PAGE buffer (Beyotime, Jiangsu, China) and boiled for 5 min. Twenty micrograms of each sample was subjected to SDS – 12% to 15% PAGE and Western blotting as previously reported [18]. Densitometric quantitation of the blotting strips was performed using Quantity-One software. GAPDH was used as an internal control. The following antibodies were used: rabbit anti-Atg7 polyclonal antibody (Abcam, ab58735, 1:2000), anti-LC3B antibody (Sigma–Aldrich, L7543, 1:1000), rabbit anti-GAPDH (14C10) mAb (Cell Signaling Technology, 2118L, 1:1000), and anti-p62/SQSTM1 antibody (Sigma–Aldrich, P0067, 1:20,000).

2.3. RNA extraction and quantitative real-time PCR

Total RNA was extracted using the TRIzol reagent (Invitrogen, 15596-026) according to the manufacturer's instructions. RNA concentration and quality were analyzed using a nucleic acid and protein analyzer (Beckman, DU640), and 1 μg of RNA was then reverse transcribed with the PrimeScript RT reagent kit (TaKaRa). Real-time quantitative PCR was performed in the Bio-Rad CFX-96 real-time PCR detection system using the following amplification parameters: 95 °C for 30 s, followed by 40 cycles of 95 °C for 5 s and 58 °C for 5 s. Relative gene expression levels were calculated as the ratio of mRNA level normalized to the level of 18S rRNA. The results were analyzed using the CFX manager software (Bio-Rad). Results were expressed as the mean ± SD of three independentexperiments. Primer sequences are listed in Supplementary Table 1.

2.4. Labeling F-actin with TRITC-phalloidin

To detect F-actin and nuclei, WT MEFs and Atg7$^{-/-}$ MEFs were grown on glass-bottomed dishes, then fixed and stained as previously reported [19]. The fluorescence images were recorded using a confocal laser scanning microscope (Zeiss, LSM 510).

2.5. Labeling of late-stage autophagosomes with monodansylcadaverine (MDC)

To detect the late-stage autophagosomes, MEFs were grown on glass-bottomed dishes. Following the indicated treatment, the cells were stained using 50 μM MDC for 10 min at 37 °C. After three washes with PBS, the cells were examined under a confocal laser scanning microscope (Zeiss, LSM 510).

For quantitative assessment of the late-stage autophagosomes after the indicated treatment, cells were subjected to MDC staining, trypsinized, collected by centrifugation, and resuspended in PBS. The cells were subjected to FACS analysis (excitation wavelength 380 nm, emission filter 525 nm) using a FACSCalibur flow cytometer.

2.6. iTRAQ labeling, sample cleaning and desalting

The iTRAQ labeling and sample cleaning was performed as described previously [20]. In this study, the WT MEFs and Atg7$^{-/-}$ MEFs were labeled with 114 and 116 iTRAQ reagents,respectively,

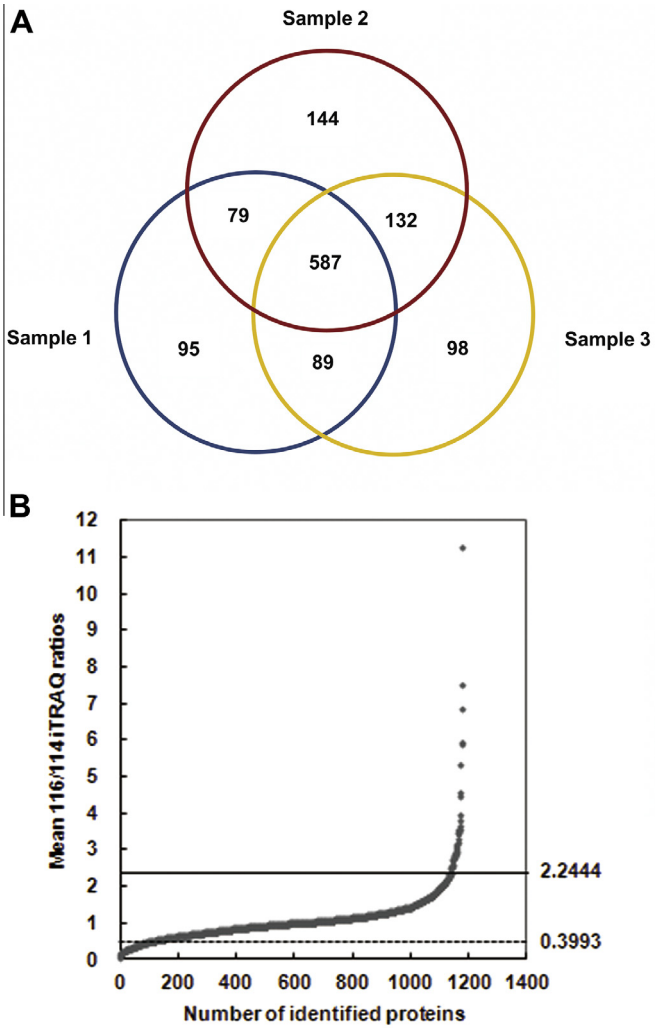

Fig. 1. Three independent iTRAQ experiments identified differentially regulated proteins in Atg7$^{-/-}$ MEFs. (A) Venn diagram depicting the overlap of proteins identified in three independent iTRAQ experiments. (B) Overall distribution of the mean protein expression ratios of 1234 proteins identified in the Atg7-deficient MEFs. The ratios were calculated by dividing the expression level of each protein in Atg7$^{-/-}$ MEFs (116) by that in WT MEFs (114). Horizontal lines in the plot indicate the 90% confidence intervals.

and three independent biological replicates were performed. Prior to the on-line 2D LC/MS/MS analysis, the iTRAQ-labeled samples were cleaned and desalted. A cation exchange cartridge system (Applied Biosystems) was used to remove the SDS reducing reagent, excess iTRAQ reagents, undigested proteins, and trypsin from the labeled sample mixture to avoid interference with the LC/MS/MS analysis.

The on-line 2D LC/MS/MS experiments were essentially performed as described previously [21]. The 2D nano-LC/MS/MS analyses were performed on a nano-HPLC system (Agilent, Waldbronn, Germany) coupled to a hybrid Q-TOF mass spectrometer (QSTAR XL, Applied Biosystems) equipped with a nano-ESI source (Applied Biosystems) and a nano-ESI tip (Picotip, New Objective Inc., Woburn, MA). The Analyst TM 1.1 software was used to control the QSTAR XL mass spectrometer and nano-HPLC system and to acquire the massspectral data.

2.7. Protein identification and relative quantitation

The raw MS data were essentially analyzed as described previously [21]. ProteinPilot Software 3.0.1 (Applied Biosystems, Software Revision Number: 67476; Applied Biosystems) was used to identify and quantify the peptides and proteins. The complete set of raw data files (*wiff) were searched against the non-redundant International Protein Index (IPI) database (mouse v3.62, 40,041 entries) using the Paragon and ProGroup algorithms (Applied Biosystems).

2.8. IPA analysis and functional categorization of differentially expressed proteins

The bioinformatics analyses of the differentiallyexpressed proteins were performed using the Ingenuity Pathways Analysis (IPA) software (version 6.3, Ingenuity Systems, http://www.ingenuity.com). The IPA software was used to assign the differentially expressed proteins to different molecular and cellular functional classes based on the underlying biological evidence obtained from the curated Ingenuity Pathways Analysis literature database. The differentially expressed proteins and their corresponding expression values were uploaded to the IPA to generate networks.

2.9. Statistical analysis

Data from the up- and down-regulated protein groups were compared using Student's *t*-tests. Each experiment was performed at least in triplicate. The results are expressed as the mean ± SD (standard deviation). The threshold for statistical significance was set at $p < 0.05$.

3. Results

3.1. Identification of differentially regulated proteins in Atg7$^{-/-}$ MEFs

In this study, we used MEFs that were deficient in Atg7, a protein that is essential for the formation of autophagosomes. The Atg7 protein was not expressed in Atg7$^{-/-}$ MEFs, and only LC3-I (one form of the mammalian homologue of Atg8) was detected in Atg7$^{-/-}$ MEFs. p62, which is preferentially degraded during autophagy, was observed to significantly accumulate in Atg7$^{-/-}$ MEFs. Together, these data show that the Atg7$^{-/-}$ MEFs displayed defective autophagy (Supplementary Fig. 1).

To identify proteins exhibiting altered expression patterns in Atg7-knockout cells, total cell lysates prepared from WT and Atg7$^{-/-}$ MEFs during log-phase growth were subjected to iTRAQ labeling and on-line 2D LC/MS/MS analyses, as described in the Materials and methods section. Three independent experiments were performed (Fig. 1A). Detailed information about the peptides and proteins identified following a search against the IPI (International Protein Index) databases for the three individual LC/MS/MS experiments is provided in Supplementary Table 2.The data from

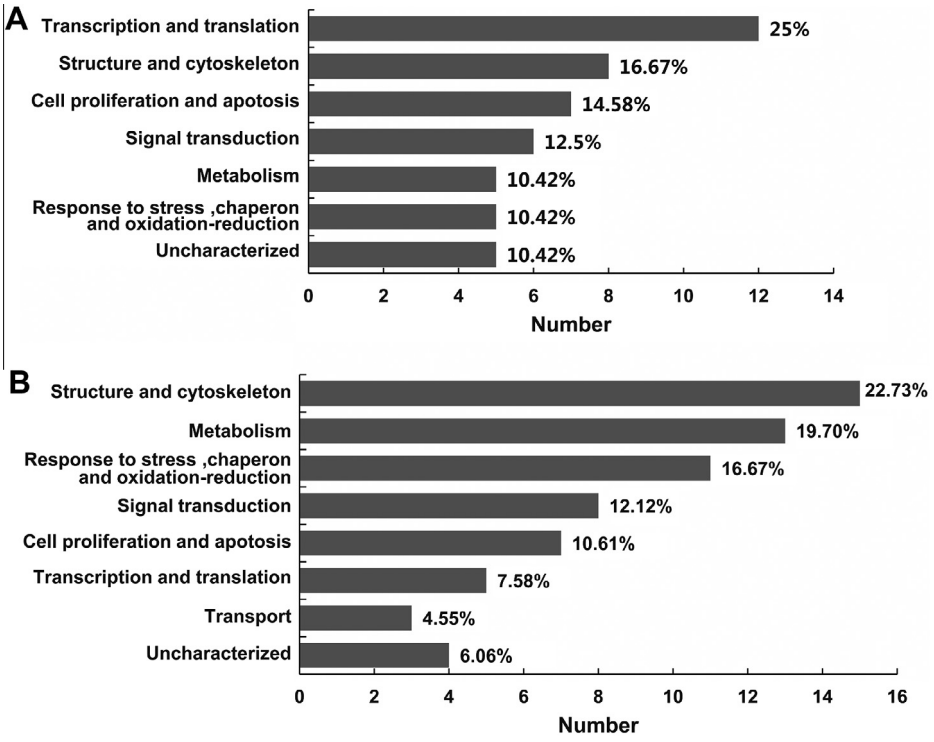

Fig. 2. Functional classification of the differentially expressed proteins in WT and Atg7$^{-/-}$ MEFs. The main biological functions of these proteins were obtained from the UniProt protein knowledge database and PubMed. (A) Up-regulated proteins. (B) Down-regulated proteins.

the three independent experiments were compared and proteins exhibiting identical accession numbers and/or gene symbols were merged. In total, 1234 non-redundant proteins were identified (Supplementary Table 3). Of these non-redundant proteins, 887 (71.88%) occurred at least twice in the three independent experiments (Fig. 1A), demonstrating that the adopted proteomics platform exhibited good reproducibility for protein identification.

The differentially expressed proteins in Atg7$^{-/-}$ MEFs were identified according to the mean 116/114 ratios of the three individual experiments, which represents the iTRAQ labeled Atg7$^{-/-}$: WT ratio. According to the criteria for identification of differentially expressed proteins, the threshold values for the down- and up-regulated proteins were $\leqslant$0.3993 and $\geqslant$2.2444 (90% confidence interval), respectively (Fig. 1B). We determined that 48 proteins were significantly up-regulated and 66 were significantly down-regulated in the Atg7$^{-/-}$ MEFs compared to the WT MEFs (Supplementary Table 4).

3.2. Functional categorization of up-regulated and down-regulated proteins

To gain insight into the biological significance of the protein expression changes in Atg7-deficient cells, the differentially expressed proteins were categorized according to their main biological functions based on information obtained from the UniProt protein knowledge database and PubMed. The 48 up-regulated proteins fell into 7 categories (Fig. 2A), and the 66 down-regulated proteins fell into 8 categories, including cell structure and cytoskeleton (22.73%) andmetabolism (19.70%) (Fig. 2B). Considering that autophagy is an intracellular pathway responsible for the degradation of long-lived proteins and entire organelles, and impaired autophagy leads to an increase in the total protein mass in the autophagy-impaired liver [15], the up-regulation of proteins in Atg7-deficient cells may result partially from impaired degradation and turnover. Therefore, we chose to further investigate the down-regulated proteins.

3.3. Protein network analysis of down-regulated proteins and the detection of F-actin in the Atg7$^{-/-}$ MEFs

To better understand interactions among the differentially expressed proteins, the 66 down-regulated proteins were uploaded into the IPA for network analysis. The networksidentified by the IPA were based on recent reports of interactions among various genes. The network of down-regulated proteins contained two obvious sub-networks centered on Hsp and F-actin (Fig. 3A). The multiple proteins involved in regulation of the actin cytoskeleton that networked in conjunction with F-actin were Plec1, Actg1, Dstn, Gsn, Actn1, Cfl1, Cfl2, Tagln, Marcks, Lima1, Akap12, and Anxa1 (Supplementary Table 5). The other sub network consisted of Hsp family members such as Hsp70, Hsp90B1, Hsp90AB1, Hsp90AA1, and Hsp (Supplementary Table 5).

In a previous study [18], we determined that F-actin was inhibited in Atg7$^{-/-}$ MEFs treated with pentagalloylglucose (PGG), a natural polyphenoliccompound that can induce autophagy in select prostate cancer cell lines. Therefore, we focused on the F-actin

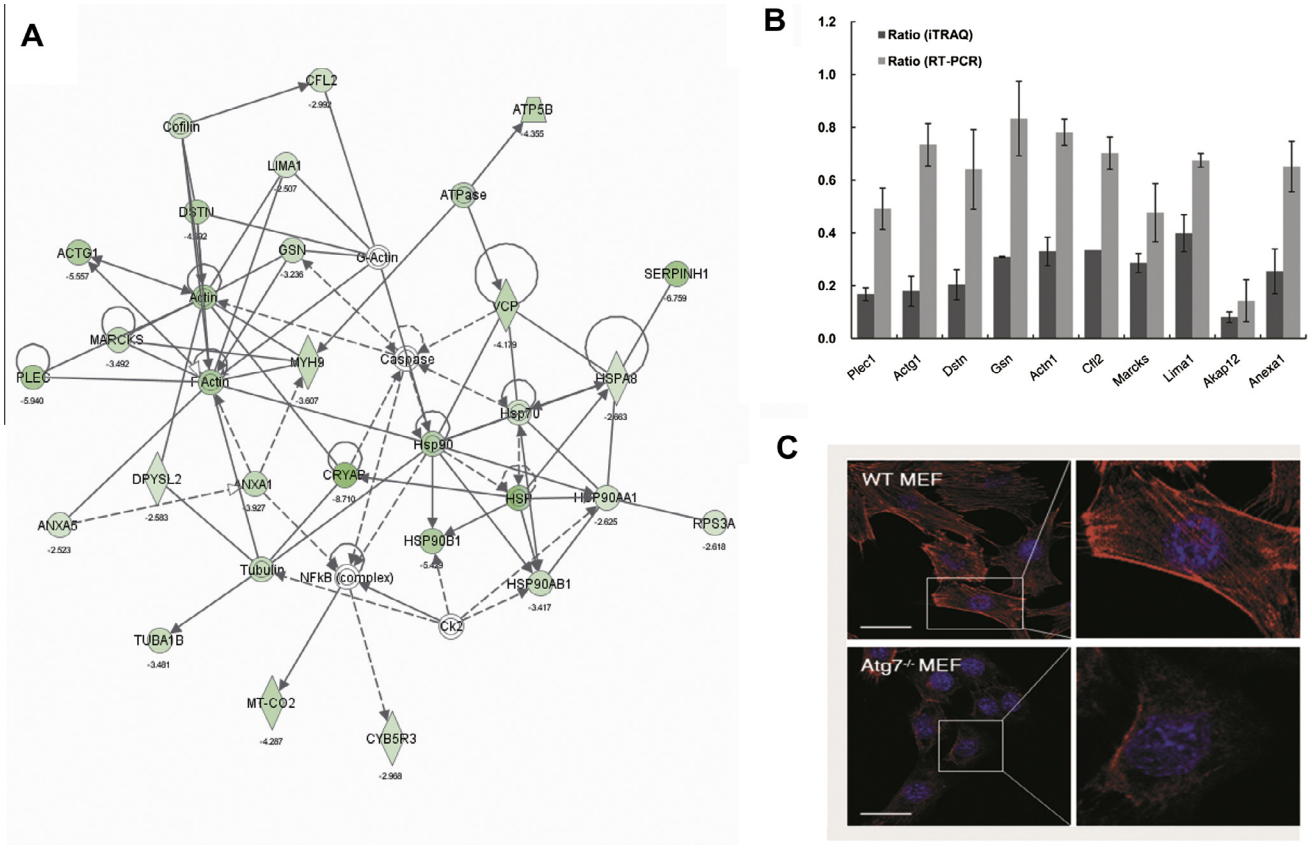

Fig. 3. Protein network analyzed down-regulated proteins and identified F-actin in the Atg7$^{-/-}$ MEFs. (A) The network of down-regulated proteins. The lines connecting proteins indicate known interrelationships found in the IPA. Direct interactions are represented by a solid line and indirect relationships are indicated by a dashed line. (B) Validation of down-regulated proteins detected using iTRAQ labeling and mass spectrometry. Real-time PCR using specific primers verified the differential expression of Plec1, Actg1, Dstn, Gsn, Actn1, Cfl1, Cfl2, Tagln, Marcks, Lima1, Akap12, and Anxa1. (C) Morphological changes in F-actin were observed in Atg7-deficient MEFs. WT and Atg7$^{-/-}$ MEFs in log-phase growth were fixed and stained for F-actin using phalloidin-TRITC and for nuclei using 4′, 6′-diamidino-2-phenylindole (DAPI) and observed under a laser scanning confocal microscope. The data are expressed as the mean ± SD of three experiments. Bars, 20 μm.

sub network. To examine F-actin in Atg7$^{-/-}$ MEFs, we first verified the downregulation of F-actin regulatory proteins using real-time PCR (Fig. 3B). The suppressed expression of these regulatory proteins suggested that regulation of F-actin was inhibited. In WT MEFs, the F-actin fibers were organized in parallel bundles; however, in Atg7$^{-/-}$ MEFs, the F-actin fibers were disorganized, and the F-actin net was loose and disassembled (Fig. 3C). Accordingly, impaired autophagy in Atg7-deficient MEFs led to morphological changes in F-actin, suggesting that autophagy affects the development of F-actin in eukaryotic cells.

3.4. Confirmation of the role ofF-actin in autophagy

We found that defective autophagy in Atg7-deficient cells impaired the expression and organization of F-actin. This finding suggests that autophagy may affect the expression and organization of F-actin. To verify the effect of F-actin on autophagosome formation, WT MEFs were pretreated with 2 μM cytochalasin D (CD) for 1 h to induce depolymerization of the existing actin filaments. Compared to the control cells, LC3-II expression was induced significantly following nutrient starvation for 1 h and a significant accumulation of autophagosomes was observed. In addition, an increased accumulation of LC3-II/GAPDH compared to the control cells was observed in the presence of 2 μM CD under both nutrient-rich and starvation conditions (Fig. 4A and B).

We next investigated the expression of p62 as an indication of autophagic flux. Under nutrient-rich conditions, the level of p62/GAPDH did not change (Fig. 4A and C), although the expression of LC3-II increased in the presence of 2 μM CD. However, compared to cells in the absence of CD under starvation conditions, we observed a significant increase in the level of p62/GAPDH in the presence of 2 μM CD. These data suggest that treatment with CD impaired autophagosome maturation. In addition, we used the acidotropic dye MDC (monodansylcadaverine) to label late-stage autophagosomes. Under nutrient-rich or starvation conditions, the number of labeled vesicles (containing green puncta) decreased, and a significant reduction in MDC fluorescence per 1×10^4 cells was observed in the presence of 2 μM CD (Fig. 4D and E). Therefore, under nutrient-rich or starvation conditions, the formation of late-stage autophagosomes was impaired in the

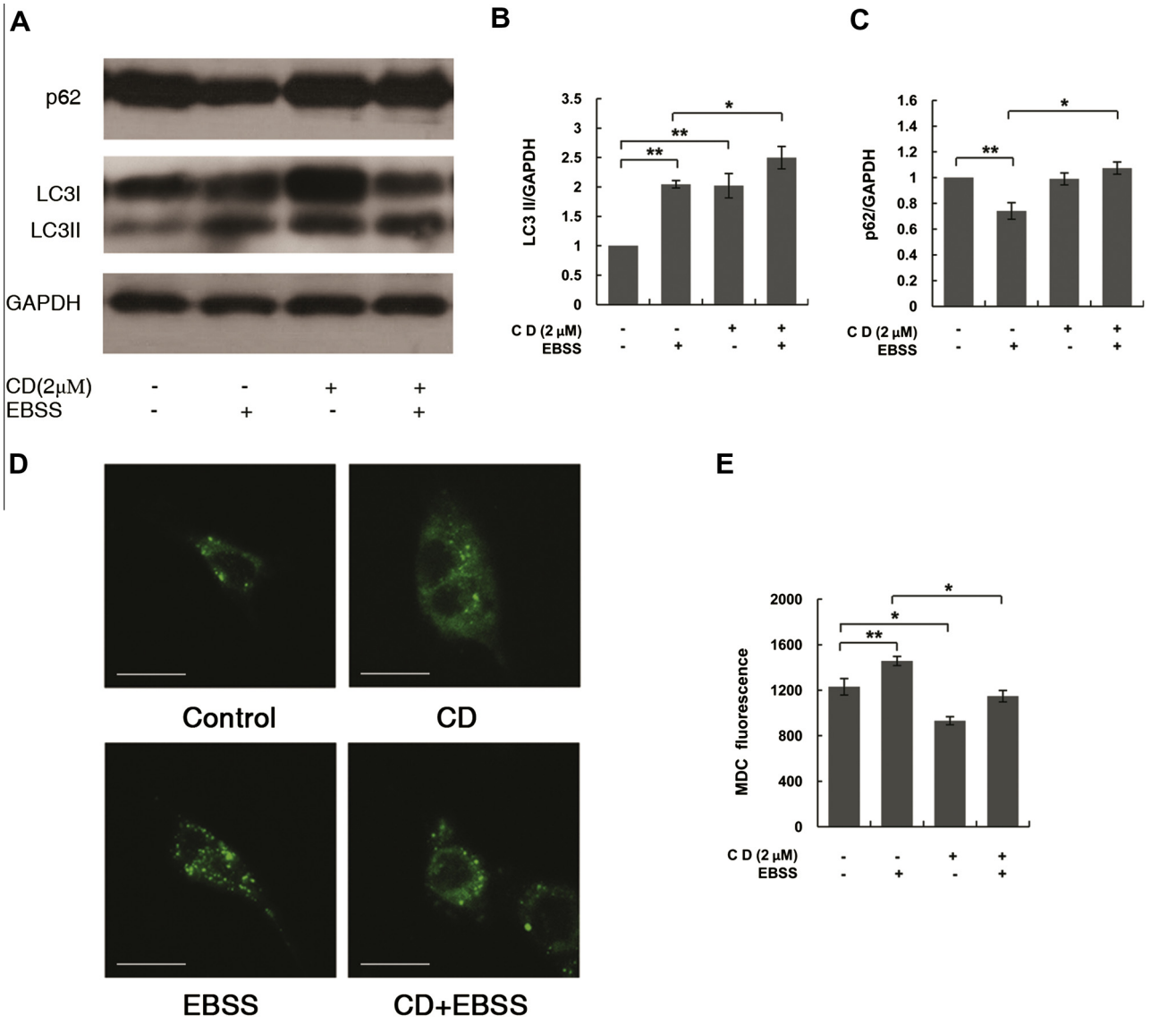

Fig. 4. Confirming the role of F-actin in autophagy. Wild-type MEFs were pre-treated with 2 μM cytochalasin D for 1 h and exposed to starvation using EBSS for 1 h. (A) LC3 levels were monitored by western blot. GAPDH was used as the loading control. Quantification of LC3-II (B) and p62 (C) levels relative to GAPDH under the experimental conditions described. (D) Late-stage autophagosomes were stained using MDC (50 μM) for 10 min at 37 °C and observed under a laser scanning confocal microscope. Bars, 20 μm. The quantification of MDC fluorescence was measured by flow cytometric analysis (E). The data are expressed as the mean ± SD of three experiments, $p < 0.05$.

presence of CD. These data suggest that an intact F-actin network plays an important role in the processes of basal and starvation-induced autophagy.

4. Discussion

In a previous report, a proteomics analysis of autophagy-deficient mouse livers demonstrated that autophagy impairment had little effect on cellular protein composition [22]. However, the proteome examined in this study was restricted to certain cell fractions; namely, the mitochondrial-lysosomal, microsomal, and cytosolic fractions. In this study, we performed a global proteomic analysis of Atg7$^{-/-}$ and WT MEFs using online 2D LC/MS/MScoupled with iTRAQ labeling. This report is the first time that proteomic differences in whole cells have been compared between Atg7$^{-/-}$ MEFs and WT MEFs and demonstrates that the proteome is larger than previously reported [22].

The protein network analysis revealed that the largest category of down-regulated proteins was structural and cytoskeletal proteins. This network contained proteins involved in actin cytoskeleton remodeling such as Plec1, Actg1, Dstn, Gsn, Actn1, Cfl1, Cfl2, Tagln, Marcks, Lima1, Akap12, and Anxa1 (Supplementary Table 5). Gsn, Cfl2 and Lima1 are actin-binding proteins (ABPs) that control different steps of the actin cytoskeleton assembly, including filament nucleation, elongation, severing, capping, and depolymerization [23]. The cofilin proteins interactwith actin dipolymers to induce depolymerization, and cofilin 1 is thought to be primarily responsible for rebuilding the actin cytoskeleton. Our previous studies indicated that cofilin 1 activation and inactivation are related to virus-induced F-actin assembly and disassembly during different phases of the HSV-1 life cycle [19]. We investigated the morphological changes in F-actin (Fig. 3C) in Atg7-deficient cells under normal conditions, and our data verified this hypothesis. Further analysis of the protein network demonstrated that F-actin was a hub for down-regulated proteins. Collectively, our findings demonstrate that autophagy can influence the expression and organization of F-actin in higher eukaryotes.

Previous studies have demonstrated the involvement of the actin cytoskeleton network in modulating autophagy [1]. Studies in yeast *Saccharomyces cerevisiae* demonstrated that the actin cytoskeleton is required for precursor Ape1 transport, and specific actin point mutants block the Cvt pathway and pexophagy without affecting normal mitochondrial morphology. In addition, actin regulates precursor Ape1 recruitment to the pre-autophagosomal structure (PAS). Thus, actin is involved in two types of selective autophagy, the Cvt pathway and pexophagy, but not in nonselective autophagy or bulk processes [1]. In this study, we performed a quantitative proteomics analysis in autophagy-deficient MEFs using iTRAQ labeling coupled with on-line 2D LC/MS/MS to demonstrate that F-actin regulation was inhibited, F-actin fibers were disorganized, and the F-actin net was loosened and disassembled in the Atg7$^{-/-}$ MEFs.

A recent study revealed that actin is necessary for starvation-mediated autophagy; M.O. Aguilera et al. found that when the actin cytoskeleton is depolymerized, the increase in autophagic vacuoles was abolished without affecting maturation of remaining autophagosomes [24]. To explore the role of F-actin in autophagy in our system, wild-type MEFs were pre-treated with 2 μM cytochalasin D for 1 h and exposed to starvation using EBSS for 1 h. We observed that autophagosomes accumulated in the presence of cytochalasin D. There are two possible explanations for the accumulation of the autophagosomes: increased autophagic activity or impaired fusion of the autophagosome vesicles, which would decrease their movement through the autophagic pathway [25]. The p62/GAPDH levels observed in the presence of cytochalasin D suggested that autophagic flux did not increase in CD-treated cells. Furthermore, the reduction in the number of labeled vesicles and in fluorescent MDC staining demonstrates that cytochalasin D blocked the formation of late-stage autophagosomes under nutrient-rich and starvation conditions. These data suggest that intact F-actin filaments facilitate the formation of late-stage autophagosomes and degradation under normal or nutrient starvation conditions. Together, these findings show that F-actin is required for both basal and starvation-induced autophagy in higher eukaryotes.

In this study, we introduced a quantitative proteomics analysis of autophagy-deficient Atg7$^{-/-}$ MEFs to identify 66 down-regulated proteins and, for the first time, demonstrated that the main down-regulated proteins were F-actin and actin-binding or actin-related proteins. Furthermore, F-actin was disassembled in the Atg7$^{-/-}$ MEFs. The treatment of WT MEFs with CD, which induces the depolymerization of F-actin, significantly impaired autophagosome maturation. Our results demonstrate a close relationship between F-actin and autophagy. However, elucidating the definitive mechanism underlying the interaction between F-actin and autophagy will require further investigation.

Acknowledgments

This work was supported by the Twelfth Five-Year National Science and Technology Support Program (2012BAI29B06), the National Natural Science Foundation of China (81274170), Jinan University's Scientific Research Creativeness Cultivation Project for Outstanding Undergraduates Recommended for Postgraduate Study, and the Major Platform Project Funds of Administration of Ocean and Fisheries of Guangdong, China (GD2012-D01-002). We thank Dr. Masaaki Komatsu (Tokyo Metropolitan Institute of Medical Science) kindly providedthe immortalised WT and Atg7-deficient mouse embryonic fibroblast cells (WT MEFs and Atg7$^{-/-}$ MEFs, respectively). We also thank Xiaogang Wang for help with the advice and guidance of this paper.

Appendix A. Supplementary data

Supplementary data associated with this article can be found, in the online version, at http://dx.doi.org/10.1016/j.bbrc.2013.06.111.

References

[1] F. Reggiori, I. Monastyrska, T. Shintani, et al., The actin cytoskeleton is required for selective types of autophagy, but not nonspecific autophagy, in the yeast *Saccharomyces cerevisiae*, Mol. Biol. Cell 16 (2005) 5843–5856.
[2] J. Huang, D.J. Klionsky, Autophagy and human disease, Cell Cycle 6 (2007) 1837–1849.
[3] V. Deretic, B. Levine, Autophagy, immunity, and microbial adaptations, Cell Host Microbe 5 (2009) 527–549.
[4] Z. Yue, S. Jin, C. Yang, et al., Beclin 1, an autophagy gene essential for early embryonic development, is a haploinsufficient tumor suppressor, Proc. Natl. Acad. Sci. USA 100 (2003) 15077–15082.
[5] M.C. Maiuri, E. Zalckvar, A. Kimchi, et al., Self-eating and self-killing: crosstalk between autophagy and apoptosis, Nat. Rev. Mol. Cell Biol. 8 (2007) 741–752.
[6] M. Tsukada, Y. Ohsumi, Isolation and characterization of autophagy-defective mutants of *Saccharomyces cerevisiae*, FEBS Lett. 333 (1993) 169–174.
[7] S. Vittorini, C. Paradiso, A. Donati, et al., The age-related accumulation of protein carbonyl in rat liver correlates with the age-related decline in liver proteolytic activities, J. Gerontol. A Biol. Sci. Med. Sci. 54 (1999) 318–323.
[8] M. Komatsu, T. Ueno, S. Waguri, Y. Uchiyama, E. Kominami, K. Tanaka, Constitutive autophagy: vital role in clearance of unfavorable proteins in neurons, Cell DeathDiffer. 14 (2007) 887–894.
[9] Z. Xie, D.J. Klionsky, Autophagosome formation: core machinery and adaptations, Nat. Cell Biol. 9 (2007) 1102–1109.
[10] N. Mizushima, T. Noda, T. Yoshimori, et al., A protein conjugation system essential for autophagy, Nature 395 (1998) 395–398.
[11] Y. Ichimura, T. Kirisako, T. Takao, et al., An ubiquitin-like system mediates protein lipidation, Nature 408 (2000) 488–492.
[12] I. Tanida, N. Mizushima, M. Kiyooka, et al., Apg7p/Cvt2p: a novel protein-activating enzyme essential for autophagy, Mol. Biol. Cell 10 (1999) 1367–1379.

[13] N. Ohsumi, Mizushima, two ubiquitin-like conjugation systems essential for autophagy, Semin. Cell Dev. Biol. 15 (2004) 231–236.
[14] S. Wiese, K.A. Reidegeld, H.E. Meyer, et al., Protein labeling by iTRAQ: a new tool for quantitative mass spectrometry in proteome research, Proteomics 7 (2007) 340–350.
[15] Komatsu, S. Waguri, T. Ueno, et al., Impairment of starvation-induced and constitutive autophagy in Atg7-deficient mice, J. Cell Biol. 169 (2005) 425–434.
[16] Y. Nishida, S. Arakawa, K. Fujitani, et al., Discovery of Atg5/Atg7-independent alternative macroautophagy, Nature 461 (2009) 654–658.
[17] J.X. Lu, Y.F. Xiang, J.X. Zhang, et al., Cloning, soluble expression, rapid purification and characterization of human Cofilin1, Protein Expr. Purif. 82 (2012) 186–191.
[18] Y. Pei, Z.P. Chen, H.Q. Ju, et al., Autophagy is involved in anti-viral activity of pentagalloylglucose (PGG) against Herpes simplex virus type 1 infection in vitro, Biochem. Biophys. Res. Commun. 405 (2011) 186–191.
[19] Y.F. Xiang, K. Zheng, H.Q. Ju, et al., Cofilin 1-mediated biphasic F-actin dynamics of neuronal cells affect herpes simplex virus 1 infection and replication, J. Virol. 86 (2012) 8440–8451.
[20] M.J. Broderick, S.J. Winder, Spectrin, alpha-actinin, and dystrophin, Adv. Protein Chem. 70 (2005) 203–246.
[21] Y.H. Ji, J.L. Ji, F.Y. Sun, et al., Quantitative proteomics analysis of chondrogenic differentiation of C3H10T1/2 mesenchymal stem cells by iTRAQ labeling coupled with on-line two-dimensional LC/MS/MS, Mol. Cell. Proteomics 9 (2010) 550–564.
[22] N. Matsumoto, J. Ezaki, M. Komatsu, et al., Comprehensive proteomics analysis of autophagy-deficient mouse liver, Biochem. Biophys. Res. Commun. 368 (2008) 643–649.
[23] S.H. Lee, R. Dominguez, Regulation of actin cytoskeleton dynamics in cells, Mol. Cells 29 (2010) 311–325.
[24] M.O. Aguilera, W. Berón, W.L. Colombo, The actin cytoskeleton participates in the early events of autophagosome formation upon starvation induced autophagy, Autophagy 8 (2012) 1590–1603.
[25] K. Castillo, D. Rojas-Rivera, F. Lisbona, et al., BAX inhibitor-1 regulates autophagy by controlling the IRE1α branch of the unfolded protein response, EMBO J. 30 (2011) 4465–4478.